Predictive Engineering Tools for Injection-Molded Long-Carbon-Fiber Thermoplastic Composites

Ba Nghiep Nguyen, Leonard S. Fifield
Pacific Northwest National Laboratory, Richland, WA 99352

Raj N. Mathur
PlastiComp, Inc., Winona, MN 55987

Seth A. Kijewski, Michael D. Sangid
Purdue University, West Lafayette, IN 47907

Jin Wang, Xiaoshi Jin, Franco Costa
Autodesk, Inc., Ithaca, NY 14850

Umesh N. Gandhi
Toyota Research Institute North America, Ann Arbor, MI 48105

Steven Mori
MAGNA Exteriors and Interiors Corp., Aurora, Ontario, Canada

Charles L. Tucker III
University of Illinois at Urbana-Champaign, Urbana, IL 61801

Project period: From October 1st 2012 to September 30th, 2014
Reporting period end date: September 30th, 2014

Quarterly report submitted to Aaron Yocum, National Energy Technology Laboratory, Morgantown, WV 26507

Pacific Northwest
NATIONAL LABORATORY

Proudly Operated by **Battelle** *Since 1965*

DISCLAIMER

Predictive Engineering Tools for Injection-molded Long-Carbon-Fiber Thermoplastic Composites

Ba Nghiep Nguyen, Leonard S. Fifield
Pacific Northwest National Laboratory, Richland, WA 99352

Raj N. Mathur, PlastiComp, Inc., Winona, MN 55987

Seth A. Kijewski, Michael D. Sangid
Purdue University, West Lafayette, IN 47907

Jin Wang, Xiaoshi Jin, Franco Costa
Autodesk, Inc., Ithaca, NY 14850

Umesh N. Gandhi, Toyota Research Institute North America,
Ann Arbor, MI 48105

Steven Mori, MAGNA Exteriors and Interiors Corp.,
Aurora, Ontario, Canada

Charles L. Tucker III, University of Illinois at Urbana-Champaign,
Urbana, IL 61801

1. Objective

The objective of this project is to advance the *predictive engineering (PE) tool* to accurately predict *fiber orientation and length distributions* in *injection-molded long-carbon fiber thermoplastic composites* for optimum design of automotive structures using these materials *to meet weight and cost reduction requirements* defined in Table 2 of DE-FOA-0000648 (Area of Interest 1).

2. Background

This project proposes to integrate, optimize and validate the fiber orientation and length distribution models previously developed and implemented in the Autodesk Simulation Moldflow Insight (ASMI) package for injection-molded long-carbon-fiber thermoplastic composites. In our previous US Department of Energy (DOE) funded project entitled: *"Engineering Property Prediction Tools for Tailored Polymer Composite Structures"* Pacific Northwest National Laboratory (PNNL), with the University of Illinois and Autodesk, Inc., developed a unique assembly of computational algorithms providing state-of-the-art process and constitutive models that enhance the capabilities of commercial software packages to predict fiber orientation and length distributions as well as subsequent mechanical properties of injection-molded long-fiber thermoplastic (LFT) composites. These predictive capabilities were validated using data generated at Oak Ridge National Laboratory on two-dimensional (2-D) structures of edge-gated plaques or center-gated disks injection-molded from long-glass-fiber/polypropylene (PP) or long-glass-fiber/polyamide 6,6 (PA66) pellets. The present effort aims at rendering the developed models more robust and efficient to automotive industry part design to achieve weight savings and cost reduction. This ultimate goal will be achieved by optimizing the developed models, improving and integrating their implementations in ASMI, and validating them for a complex three-dimensional (3D) long-carbon fiber (LCF) thermoplastic automotive part. Both PP and PA66 are used for the resin matrices. Local fiber orientation and length distributions at the key regions on the part are measured for the model validation based on the 15% accuracy criterion. The project outcome will be the ASMI package enhanced with computational capabilities to accurately predict fiber orientation and length distributions in automotive parts designed with long-carbon fiber thermoplastics.

3. Accomplishments

During the last quarter of FY 2014, the following technical progress has been made toward project milestones:

1) Autodesk, Inc. (Autodesk) has implemented a new fiber length distribution (FLD) model based on an unbreakable length assumption with Reduced Order Modeling (ROM) by the Proper Orthogonal Decomposition (POD) approach in the mid-plane, dual-domain and 3D solvers.

2) Autodesk improved the ASMI 3D solver for fiber orientation prediction using the anisotropic rotary diffusion (ARD) – reduced strain closure (RSC) model.

3) Autodesk received consultant services from Prof. C.L. Tucker at the University of Illinois on numerical simulation of fiber orientation and fiber length.

4) PlastiComp, Inc. (PlastiComp) suggested to Purdue University a procedure for fiber separation using an inert-gas atmosphere in the burn-off furnace.

5) Purdue University hosted a face-to-face project review meeting at Purdue University on August 6-7, 2014.

6) Purdue University (Purdue) conducted fiber orientation measurements for 3 PlastiComp plaques: fast-fill 30wt% LCF/PP edged-gated, slow-fill 50wt% LCF/PP edge-gated, and slow-fill 50wt% LCF/PP center-gated plaques, and delivered the orientation data for these plaques at the selected locations (named A, B, and C) to PNNL.

7) PNNL conducted ASMI mid-plane analyses for the above PlastiComp plaques and compared the predicted fiber orientations with the measured data provided by Purdue at Locations A, B, and C (Figure 1) on these plaques.
8) PNNL planned the project review meeting (August 6-7, 2014) with Purdue.
9) PNNL performed ASMI analyses for the Toyota complex parts with and without ribs, having different wall thicknesses, and using the PlastiComp 50wt% LCF/PP, 50wt% LCF/PA66, 30wt% LCF/PP, and 30wt% LCF/PA66 materials to provide guidance for tool design and modifications needed for molding these parts.
10) Magna Exteriors and Interiors Corp. (Magna) molded plaques from the 50% LCF/PP and 50% LCF/PA66 materials received from Plasticomp in order to extract machine purgings (purge materials) from Magna's 200-Ton Injection Molding machine targeted to mold the complex part.
11) Toyota and Magna discussed with PNNL tool modification for molding the complex part.

Figure 1. Regions A, B and C defined on the edge-gated (left) and center-gated (right) plaques where samples were cut out for fiber orientation and length measurements.

4. Progress and Status

4.1 Fiber Orientation and Length Characterization (Purdue)

Purdue hosted the face-to-face project review meeting on August 6-7, 2014 on campus at Purdue. Presentations were made on the methodology for fiber orientation and length characterization at the review meeting. Purdue completed and reported the following sets of orientation data:

- Fast-fill 30wt% LCF/PP edge-gated plaque, locations A, B and C
- Slow-fill 50wt% LCF/PP edge-gated plaque, locations A, B and C
- Slow-fill 50wt% LCF/PP center-gated plaque, locations A, B and C

In continuing to explore the fiber length characterization procedure, Purdue performed length measurements on fiber pellets and four sets of purge material including Plasticomp and Autodesk slow-fill 50wt% LCF/PA66 and slow-fill 50wt% LCF/PP. Also, a sensitivity analysis was completed on the number of fibers necessary for a statistically representative sample size.

It was noted that the fiber tips were breaking off due to oxidation of the fibers. Other protocols for matrix burn off in air were explored, and a design of experiments was performed to investigate the oven time and temperature.

4.2 Suggestion of a Procedure for Fiber Separation (PlastiComp)

PlastiComp participated in the project review meeting held at Purdue University on August 6-7, 2014. During the course of various presentations, and especially fiber-length measurements at Purdue, the data seemed to suggest that the fibers were oxidized during separation from the polyamide matrix. The markers of the suspected oxidation were:

- Fiber diameter reduction from a nominal 7 μm to 5 μm,
- A sharpening of fibers, indicative of accelerated oxidation at fiber tips,
- Dusting, indicative of fiber milling,
- Fiber-length averages substantially below 2 mm.

The oxidation of fibers is related to the lack of an inert-gas atmosphere in the burn-off furnace. As oxidized fibers are not a true representation of the fiber-lengths in the composite, PlastiComp has recommended controlled burn-off in inert gas (nitrogen) gas flow (Figure 1). PlastiComp also conveyed a schematic of the equipment required, equipment identification and estimated costs.

In view of program timelines, an alternative fiber recovery procedure to the furnace resin burn-off was suggested by PlastiComp. The alternative procedure, acid digestion, is suitable for carbon-fiber reinforced polyamides and involves dissolving samples in 98% concentration formic acid, filtering through 2 μm paper, and collecting the fibers. This method will not work for the equivalent polypropylene composites. A second limitation to this alternative method is that the dissolution technique cannot retain the original fiber locations in the sample, thus leading to bias in fiber-length vs. location in the samples.
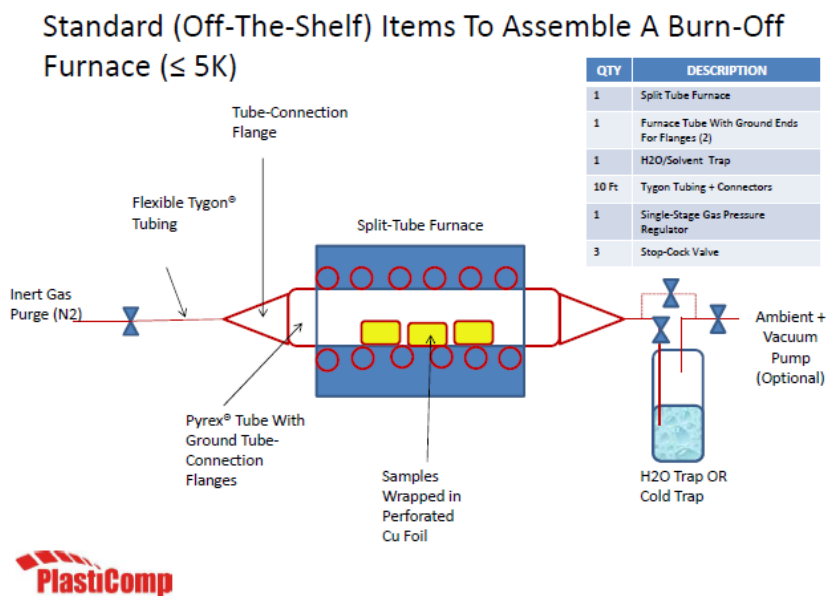

Figure 2. Schematic of the inert-gas atmosphere burn-off procedure suggested by PlastiComp.

4.3 Process Modeling of PlastiComp Plaques Using ASMI (PNNL)

PNNL received three sets of fiber orientation data from Purdue for the samples at locations A, B and C (Figure 1) of the PlastiComp plaques listed in Section 4.1. These samples were cut from the fast-fill 30wt% LCF/PP edge-gated, slow-fill 50wt% LCF/PP edge-gated, and slow-fill 50wt% LCF/PP center-gated plaques. On discussion with Autodesk, PNNL used this data to conduct the validation of ASMI fiber orientation prediction. From the measured data, a target fiber orientation tensor, A_{ij}, was selected, and from this target, a set of acceptable b_i parameters for the anisotropic rotary diffusion reduced strain closure (ARD-RSC) model [1-2] were identified. The b_i parameters were identified following the procedure proposed by Phelps et al. [1-2], by fitting the steady-state solution in a simple shear flow to the selected target orientation and requiring physically valid fiber interaction tensor **C** in all flows and stable transient orientation solutions in simple shear as well as planar, uniaxial, and biaxial elongation flows. The target steady-state fiber orientation of the model was chosen based on the measured orientation in the shell layers. The ASMI simulations used the actual process parameters that PlastiComp used when molding the plaques. The b_i and reduced strain closure *RSC* parameters identified for the 30wt% LCF/PP fast-fill molding are:

b_1 = -0.002074, b_2 = 0.1512, b_3 = 0, b_4 = 0.01209   , b_5 = 0 , *RSC*=0.008,

and those for the slow-fill 50wt% LCF/PP are:

b_1 = 0.001654, b_2 = 0.0054, b_3 = 0.025 , b_4 = -0.0008676   , b_5 = – 0.005   , *RSC*=0.02

Figure 3 shows the ASMI finite element models for the edge-gated and center-gated plaques used in the analyses.
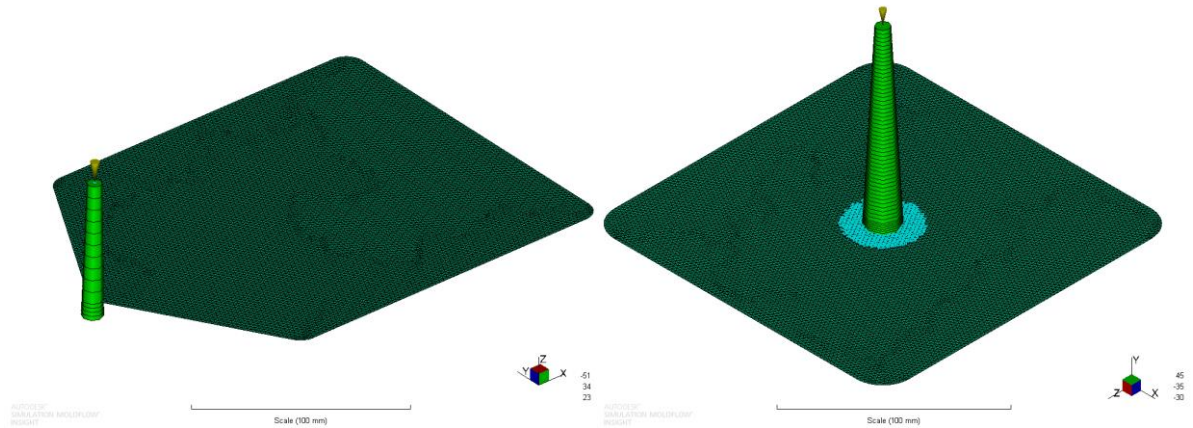

Figure 3. ASMI models for the PlastiComp edge-gated plaque (left) and center-gated plaque (right).

<u>*Evaluation of the 15% accuracy criterion*</u>

As fiber orientation strongly varies through the sample thickness, it is not possible and meaningful to have the point-by-point comparisons between the predicted and measured fiber orientations for all the components of the second-order fiber orientation tensor. Instead, a quantitative method for comparing measured and predicted fiber orientations using the calculated mechanical properties as the basis for assessing the accuracy in fiber orientation prediction is meaningful and relevant. In this work, the tensile elastic moduli and flexural moduli computed for the flow and cross-flow directions using predicted and measured fiber orientations were used to evaluate whether the ASMI fiber orientation prediction at a given location agrees with the measured data within 15%.

For the tensile elastic moduli, the injection-molded composite at a given location (A, B or C) is modeled as a laminated composite whose layers are assigned fiber orientation according to the predicted or measured fiber orientation results. Next, stiffness averaging was used to predict the linear elastic stiffness tensor of each layer in terms of predicted or measured fiber orientation according to [3]:

$$\overline{H}_{ijkl} = B_1 \tilde{A}_{ijkl} + B_2 (A_{ij}\delta_{kl} + A_{kl}\delta_{ij}) + B_3 (A_{ik}\delta_{jl} + A_{il}\delta_{jk} + A_{jl}\delta_{ik} + A_{jk}\delta_{il})$$
$$+ B_4 \delta_{ij}\delta_{kl} + B_5 (\delta_{ik}\delta_{jl} + \delta_{il}\delta_{jk}) \tag{1}$$

where the coefficients B_i ($i = 1, 5$) are the invariants of the stiffness tensor of the unidirectional transversely isotropic composite. A_{ij} and $\tilde{A}_{ijkl}$ are the second and fourth-order orientation tensors, respectively, and δ_{ij} is the identity tensor. From Eq. (1), the flow- and cross-flow direction elastic moduli were computed. The elastic moduli for the whole laminate based on predicted and measured orientation should match within 15%.

Similarly, the flexural moduli were also computed using lamination theory as

$$D_{ij} = \frac{1}{3}\sum_{k=1}^{n} \overline{H}_{ij}^{k} (z_k^3 - z_{k-1}^3) \tag{2}$$

where $\overline{H}_{ij}^{k}$ is given in Eq. (1) with the use of contracted notations, and coordinates z_k ($k =1, ...,n$) indicate the layer positions along the thickness direction (z-direction). The principal flexural moduli, D_{11} and D_{22} based on predicted and measured orientation should match within 15%.

The elastic properties for the carbon fiber adopted in the computations were: longitudinal modulus, E_L = 230 GPa, transverse modulus, E_T = 13.8 GPa, longitudinal shear modulus, G_L = 12.4 GPa, longitudinal aspect ratio, v_L = 0.2, and transverse aspect ratio v_T = 0.25. The assumed elastic modulus and Poisson's ratio of polypropylene were 1.7 GPa and 0.4, respectively. A uniform fiber aspect ratio, l/d = 200 was also assumed in the computation.

Results for the fast-fill 30wt% LCF/PP edge-gated plaque

Figures 4 to 6 show the predicted and measured through-thickness evolutions of the orientation components A_{11} (flow-direction) and A_{22} (cross-flow direction) at locations A, B and C on this plaque. A globally good agreement in trend and values were found for all three locations. Tables 1 and 2 show good agreements in modulus predictions using predicted and measured fiber orientations. The 15% accuracy criterion is satisfied based on tensile moduli. Tables 3 and 4 show globally good agreement in flexural modulus predictions except for D_{11} at location B that was beyond 15%.

Results for the slow-fill 50wt% LCF/PP edge-gated plaque

Figures 7 to 9 show the predicted and measured through-thickness evolution of the orientation components A_{11} and A_{22} at locations A, B and C on this plaque. The experimental fiber orientation data show that the core is very large at location A, and becomes progressively narrower from A to C. ASMI captured this experimental tendency well as shown in Figures 7 to 9. Good global agreement was found in the trends and values for all three locations. Tables 5 and 6 show reasonable agreement in modulus predictions using predicted and measured fiber orientation. The 15% accuracy criterion is satisfied based

on tensile moduli except for E_{11} at location C that was beyond 15%. Tables 7 and 8 show good global agreement in flexural modulus predictions apart from D_{22} at location A that was beyond 15%.

Results for the slow-fill 50wt% LCF/PP center-gated plaque

Figures 10 to 12 show the predicted and measured through-thickness evolution of the orientation components A_{11} and A_{22} at locations A, B and C on this plaque. As observed for the edge-gated plaque molded from the same material, the experimental fiber orientation data show that the core is very large at location A, and becomes progressively narrower from A to C. ASMI well captures this experimental tendency as shown in Figures 10 to 12. The 15% accuracy criterion is satisfied based on tensile moduli apart from E_{11} at location C that was beyond 15% (Tables 9 and 10). Tables 11 and 12 show good global agreement in flexural modulus predictions except for D_{22} at location A that was beyond 15%.
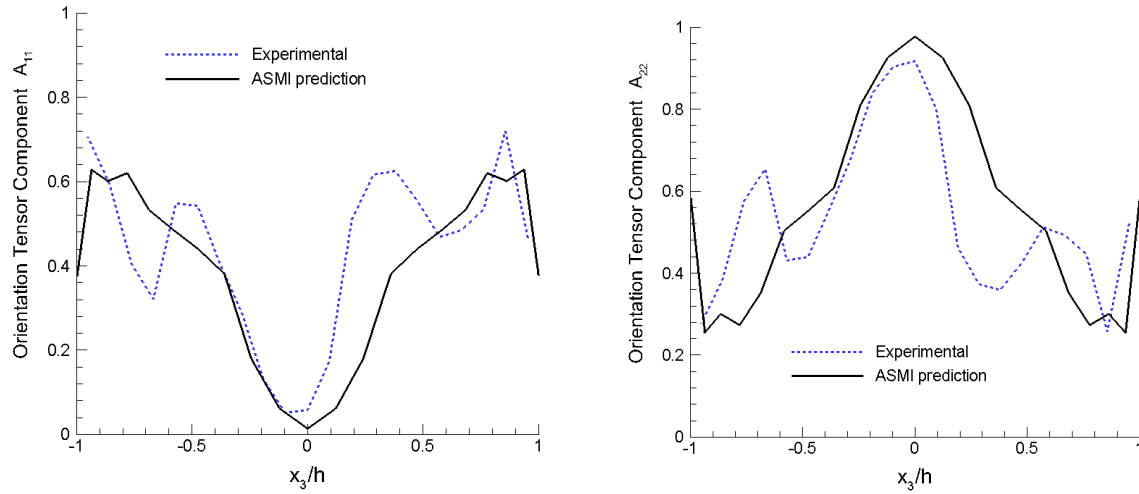

Figure 4. Predicted and measured fiber orientation tensor components in the flow- and cross-flow directions: (left) A_{11}, (right) A_{22}, for the edge-gated fast-fill 30wt% LCF/PP plaque at location A.

Figure 5. Predicted and measured fiber orientation tensor components in the flow- and cross-flow directions: (left) A_{11}, (right) A_{22}, for the edge-gated fast-fill 30wt% LCF/PP plaque at location B.

Figure 6. Predicted and measured fiber orientation tensor components in the flow- and cross-flow directions: (left) A_{11}, (right) A_{22}, for the edge-gated fast-fill 30wt% LCF/PP plaque at location C.
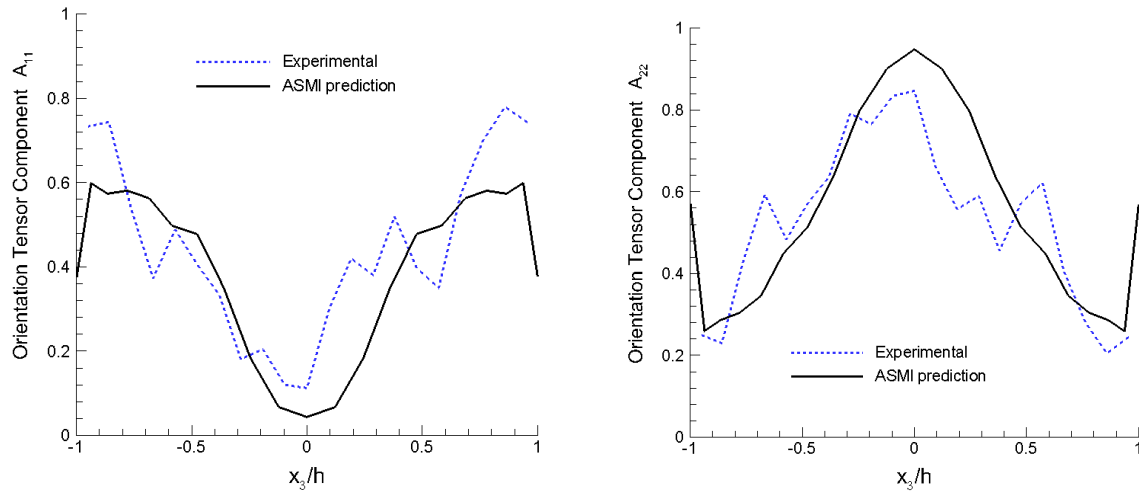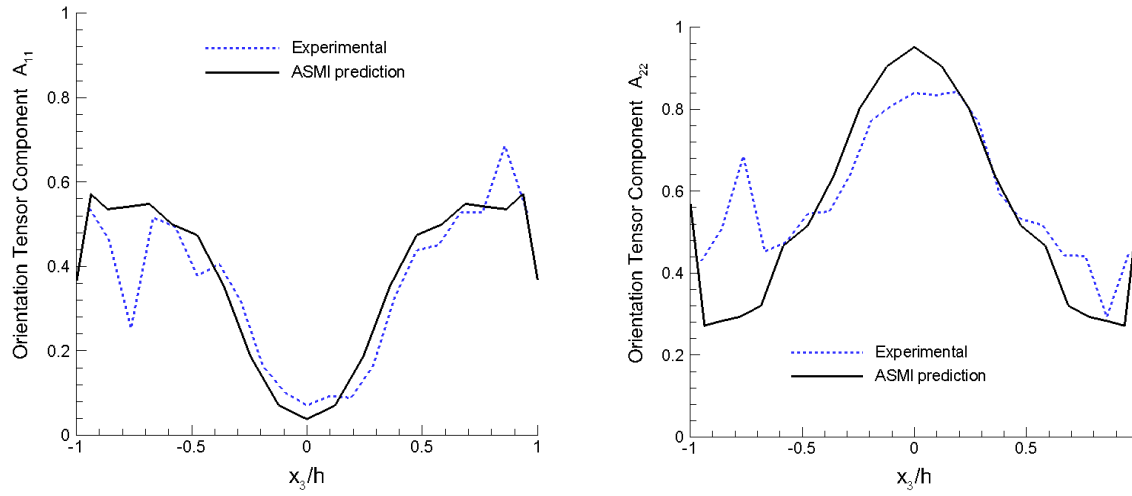
Tensile Modulus	E_{11} (predicted orientation) MPa	E_{11} (measured orientation) MPa	Agreement within
Loc. A	14382	15791	8.9%
Loc. B	14001	16127	13.2%
Loc. C	13360	12573	6.3%

Table 1. Computed E_{11} based on predicted and measured fiber orientations at locations A, B, and C in the edge-gated fast-fill 30wt% LCF/PP plaque.

Tensile Modulus	E_{22} (predicted orientation) MPa	E_{22} (measured orientation) MPa	Agreement within
Loc. A	20300	19819	2.4%
Loc. B	19638	19305	1.7%
Loc. C	19669	21665	9.2%

Table 2. Computed E_{22} based on predicted and measured fiber orientations at locations A, B, and C in the edge-gated fast-fill 30wt% LCF/PP plaque.

Flexural Modulus	D_{11} (predicted orientation) MPa.mm3	D_{11} (measured orientation) MPa.mm3	Agreement within
Loc. A	25794	28483	9.44%
Loc. B	25479	33002	22.8%
Loc. C	24644	25202	2.21%

Table 3. Computed D_{11} based on predicted and measured fiber orientations at locations A, B, and C in the edge-gated fast-fill 30wt% LCF/PP plaque.

Flexural Modulus	D_{22} (predicted orientation) MPa.mm3	D_{22} (measured orientation) MPa.mm3	Agreement within
Loc. A	36788	35557	3.46%
Loc. B	35823	31575	13.45%
Loc. C	35818	37038	3.29%

Table 4. Computed D_{22} based on predicted and measured fiber orientations at locations A, B, and C in the edge-gated fast-fill 30wt% LCF/PP plaque.
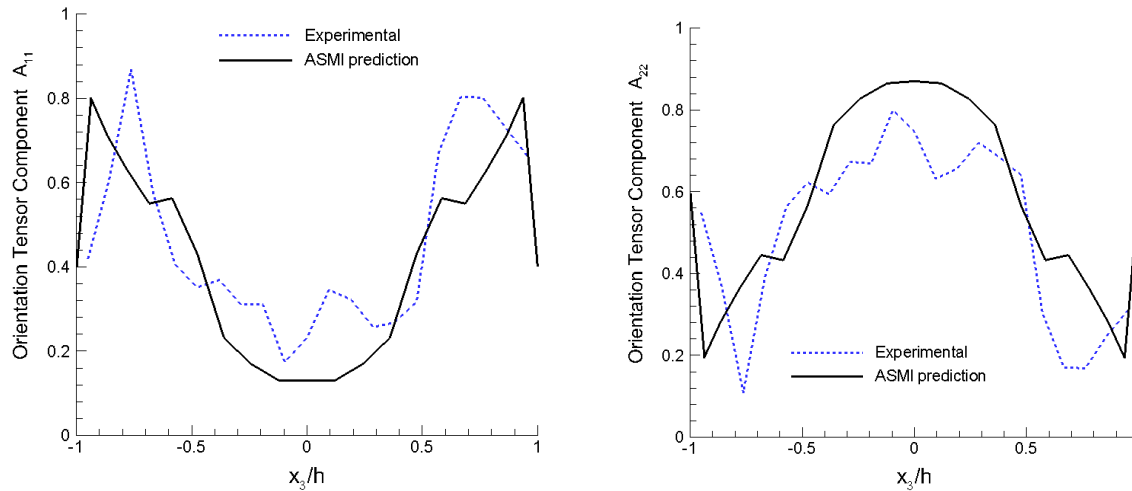

Figure 7. Predicted and measured fiber orientation tensor components in the flow- and cross-flow directions: (left) A_{11}, (right) A_{22}, for the edge-gated slow-fill 50wt% LCF/PP plaque at location A.

Figure 8. Predicted and measured fiber orientation tensor components in the flow- and cross-flow directions: (left) A_{11}, (right) A_{22}, for the edge-gated slow-fill 50wt% LCF/PP plaque at location B.

Figure 9. Predicted and measured fiber orientation tensor components in the flow- and cross-flow directions: (left) A_{11}, (right) A_{22}, for the edge-gated slow-fill 50wt% LCF/PP plaque at location C.
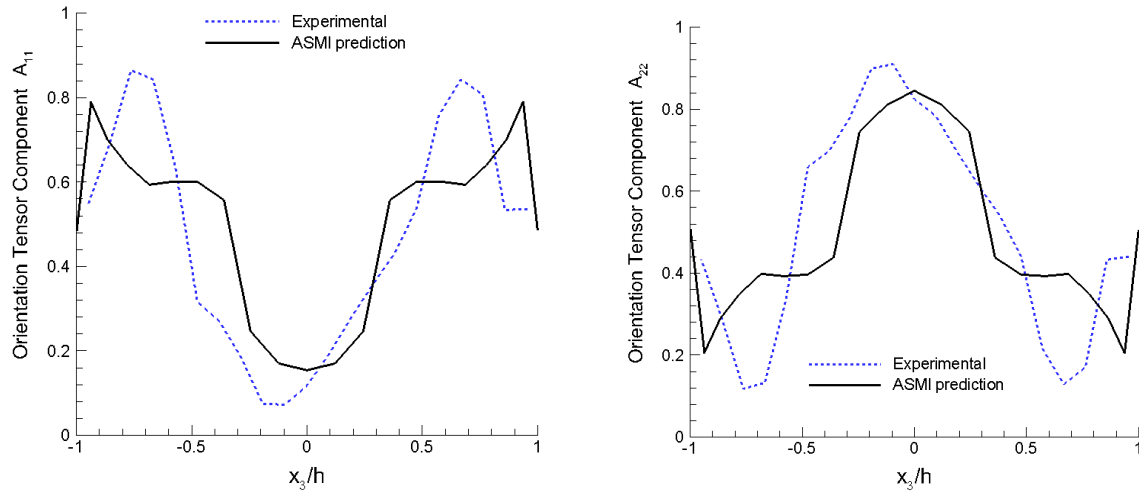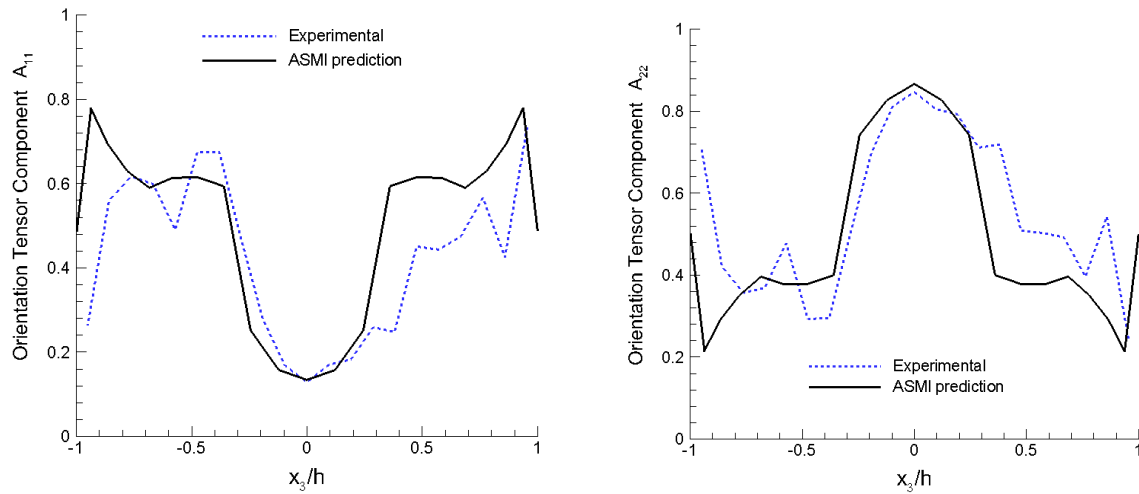
Tensile Modulus	E_{11} (predicted orientation) MPa	E_{11} (measured orientation) MPa	Agreement within
Loc. A	29699	29501	0.67%
Loc. B	34367	32037	7.27%
Loc. C	34478	26347	30.86%

Table 5. Computed E_{11} based on predicted and measured fiber orientations at locations A, B, and C in the edge-gated slow-fill 50wt% LCF/PP plaque.

9

Tensile Modulus	E_{22} (predicted orientation) MPa	E_{22} (measured orientation) MPa	Agreement within
Loc. A	37681	33319	13.09%
Loc. B	30827	34402	10.39%
Loc. C	30589	35982	14.99%

Table 6. Computed E_{22} based on predicted and measured fiber orientations at locations A, B, and C in the edge-gated slow-fill 50wt% LCF/PP plaque.

Flexural Modulus	D_{11} (predicted orientation) MPa.mm3	D_{11} (measured orientation) MPa.mm3	Agreement within
Loc. A	48495	56419	14.04%
Loc. B	56854	54405	4.5%
Loc. C	57042	53729	6.17%

Table 7. Computed D_{11} based on predicted and measured fiber orientations at locations A, B, and C in the edge-gated slow-fill 50wt% LCF/PP plaque.

Flexural Modulus	D_{22} (predicted orientation) MPa.mm3	D_{22} (measured orientation) MPa.mm3	Agreement within
Loc. A	65166	53168	22.57%
Loc. B	54607	56893	1.81%
Loc. C	54215	56025	0.37%

Table 8. Computed D_{22} based on predicted and measured fiber orientations at locations A, B, and C in the edge-gated slow-fill 50wt% LCF/PP plaque.
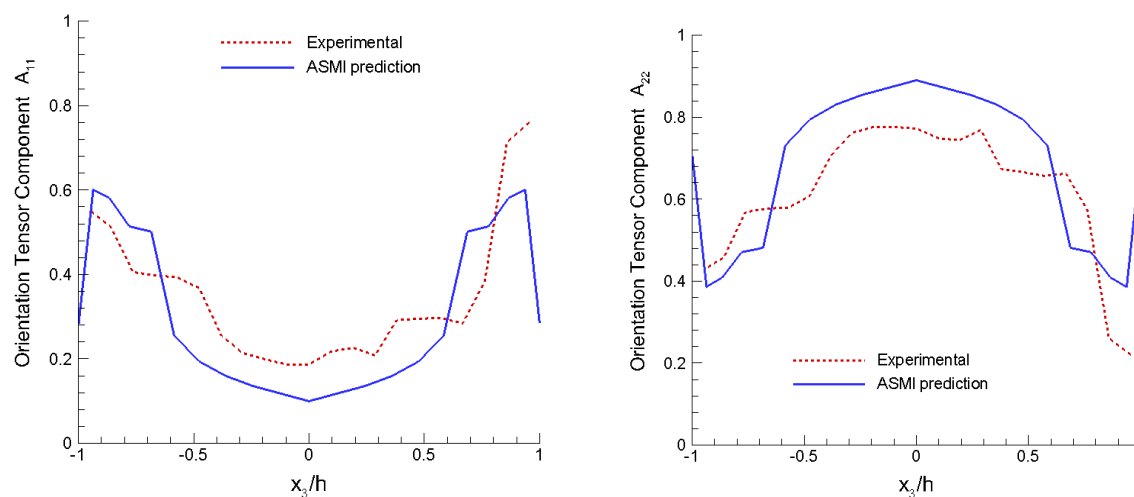
Figure 10. Predicted and measured fiber orientation tensor components in the flow- and cross-flow directions: (left) A_{11}, (right) A_{22}, for the center-gated slow-fill 50wt% LCF/PP plaque at location A.

Figure 11. Predicted and measured fiber orientation tensor components in the flow- and cross-flow directions: (left) A_{11}, (right) A_{22}, for the center-gated slow-fill 50wt% LCF/PP plaque at location B.

Figure 12. Predicted and measured fiber orientation tensor components in the flow- and cross-flow directions: (left) A_{11}, (right) A_{22}, for the center-gated slow-fill 50wt% LCF/PP plaque at location C.
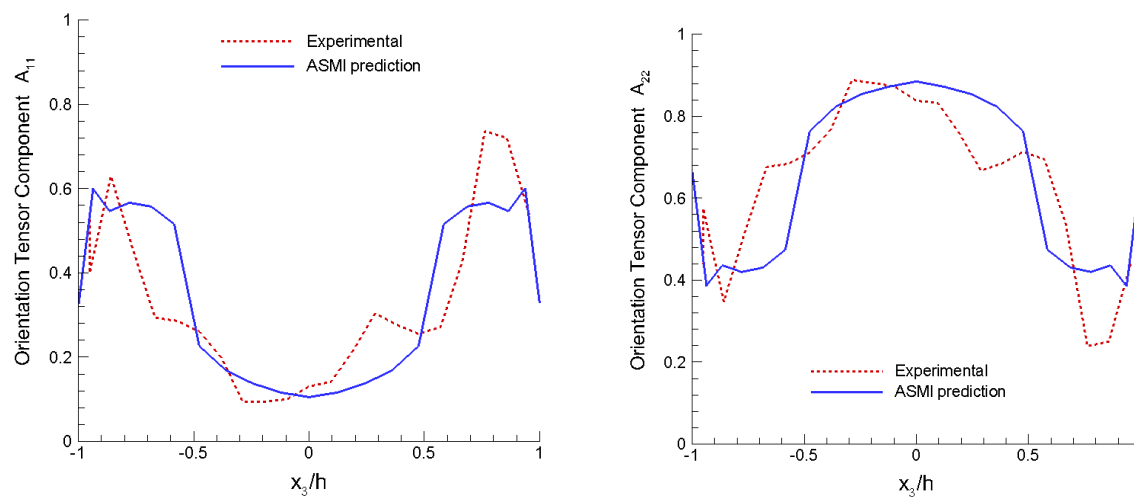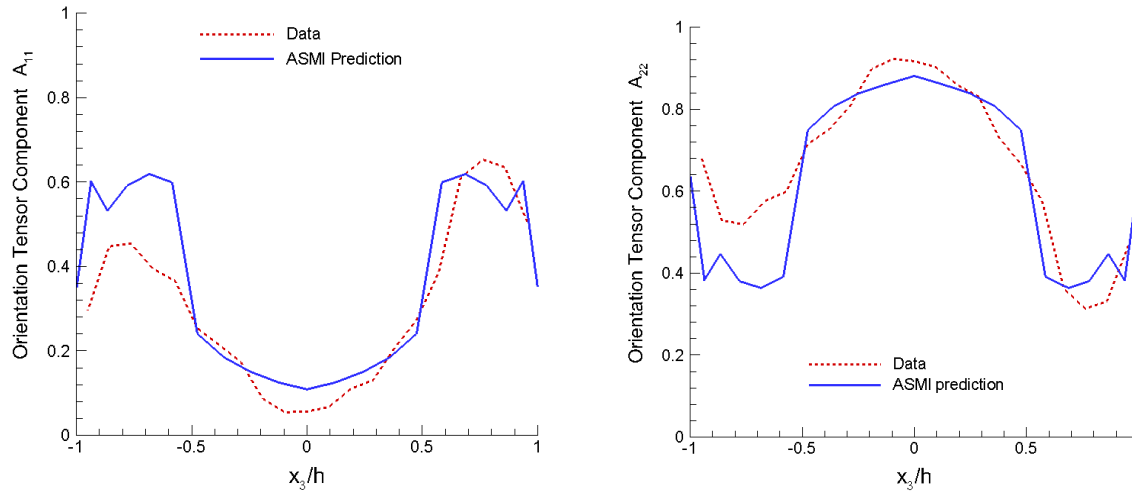
Tensile Modulus	E_{11} (predicted orientation) MPa	E_{11} (measured orientation) MPa	Agreement within
Loc. A	20626	21174	2.59%
Loc. B	23293	20322	14.62%
Loc. C	24895	18928	31.52%

Table 9. Computed E_{11} based on predicted and measured fiber orientations at locations A, B, and C in the center-gated slow-fill 50wt% LCF/PP plaque.

Tensile Modulus	E_{22} (predicted orientation) MPa	E_{22} (measured orientation) MPa	Agreement within
Loc. A	46553	41332	12.63%
Loc. B	43175	44762	3.55%
Loc. C	41155	46432	11.37%

Table 10. Computed E_{22} based on predicted and measured fiber orientations at locations A, B, and C in the center-gated slow-fill 50wt% LCF/PP plaque.

Flexural Modulus	D_{11} (predicted orientation) MPa.mm3	D_{11} (measured orientation) MPa.mm3	Agreement within
Loc. A	34727	47938	27.56%
Loc. B	38997	40297	3.23%
Loc. C	41539	37555	10.61%

Table 11. Computed D_{11} based on predicted and measured fiber orientations at locations A, B, and C in the center-gated slow-fill 50wt% LCF/PP plaque.

Flexural Modulus	D_{22} (predicted orientation) MPa.mm3	D_{22} (measured orientation) MPa.mm3	Agreement within
Loc. A	79576	62281	27.77%
Loc. B	74230	70461	5.35%
Loc. C	70899	73415	3.43%

Table 12. Computed D_{22} based on predicted and measured fiber orientations at locations A, B, and C in the center-gated slow-fill 50wt% LCF/PP plaque.

4.4 Complex Part Mold Filling Pre-Analysis (PNNL)

PNNL completed the milestone on "*filling analysis on the 3D part for determining the minimum wall thickness for cavity filling and maximizing the average fiber length to exceed 1-2mm.*" A formal milestone report was provided to the US DOE [4]. This section summarizes the work in that milestone report [4]. Four PlastiComp materials adopted for the project were used in the mold filling pre-analysis for the Toyota complex part: 30wt% LCF/ PP, 30wt% LCF/PA66, 50wt% LCF/PP and 50wt% LCF/PA66. These materials had been characterized by Autodesk, Inc. and the rheological and physical data were provided to PNNL for the process simulations using ASMI. A first round of mold filling pre-analyses had been conducted for the complex part considering 50wt% LCF/PP and 50wt% LCF/PA66 materials as the 50wt% carbon fiber loading was initially adopted for the complex part. The first pre-analysis results indicated that it is difficult to achieve mold filling of the 50wt% LCF/PA66 part and the pressure at the end of fill predicted for the 2-mm wall thickness part attained very high values. Therefore, after discussions with the team, 30wt% fiber loading was adopted, and it was suggested to consider 2.8 mm and 3.0 mm wall thicknesses for the part so that when the project enters Phase 2 the tool could be used for fiber loading values higher than 30wt% as needed. At the time of this report, the FLD data for the purge materials is not available. Therefore, based on a discussion with PlastiComp, *a weight average length of 4 mm for fibers in the charge at the injection molding machine nozzle is a reasonable assumption and was used in the analyses as the fiber length inlet condition.*

The following conclusions can be drawn from the pre-analysis [4]:

1) It appears that successful molding of the complex part with 50wt% LCF/PA66 would be difficult to achieve in practice due to high pressures in the part during filling. Reducing the wall thickness to 2 mm would significantly increase the pressure in the part and exacerbate molding issues. The molding difficulty with 50wt% LCF/PA66 is due to the high viscosity of this material at the considered molding conditions. Figures 1 to 4 show that 50wt% LCF/PA66 has the highest viscosity of the materials investigated in the range of shear rates considered.

2) It would be easier to mold 50wt% LCF/PP than 50wt% LCF/PA66.

3) ASMI predicted successful mold fillings of the complex part using both 30wt% LCF/PP and 30wt% LCF/PA66, for all the wall thicknesses considered: 2.0 mm, 2.8 mm and 3.0 mm, and for complex parts both with ribs and without ribs.

4) Wall thickness considered for the complex part should be between 2.8 mm to 3.0 mm so that the tool used to build the complex part can be used not only for 30wt% fiber loading but higher fiber loadings as well.

5) Assuming 4-mm fiber length as the fiber length inlet condition, ASMI predicted weight-average lengths significantly exceeding the 1-2 mm range for the various locations selected on the parts filled with 30wt% LCF/PP and 30wt% LCF/PA66.

Figures 13 to 18 present the analysis results for the 30wt% LCF/PP and 30wt% LCF/PA66 complex parts *with ribs* and having *2.8-mm* wall thickness. ASMI predicted successful mold filling for these parts. Acceptable and lower levels of pressure at the end of fill were found for both materials compared to the similar 2-mm wall thickness parts, and the fillings were completed within realistic fill times that could be achieved in practice. In addition, for the various locations selected on the parts, the predicted weight-average lengths significantly exceeded the 1-2 mm range.
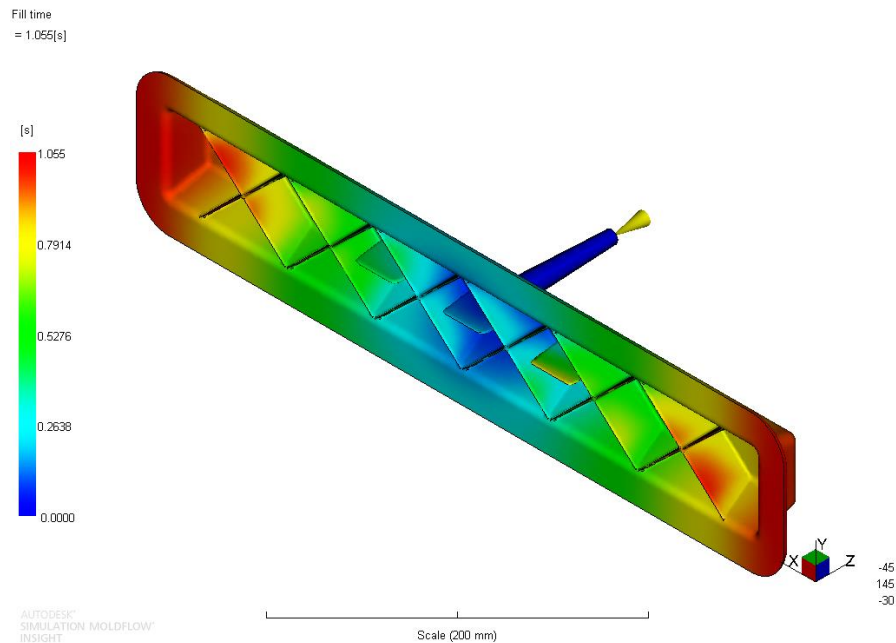

Figure 13. Fill time predicted for the 2.8-mm, 30wt% LCF/PA66 complex part with ribs – successful mold filling was predicted.
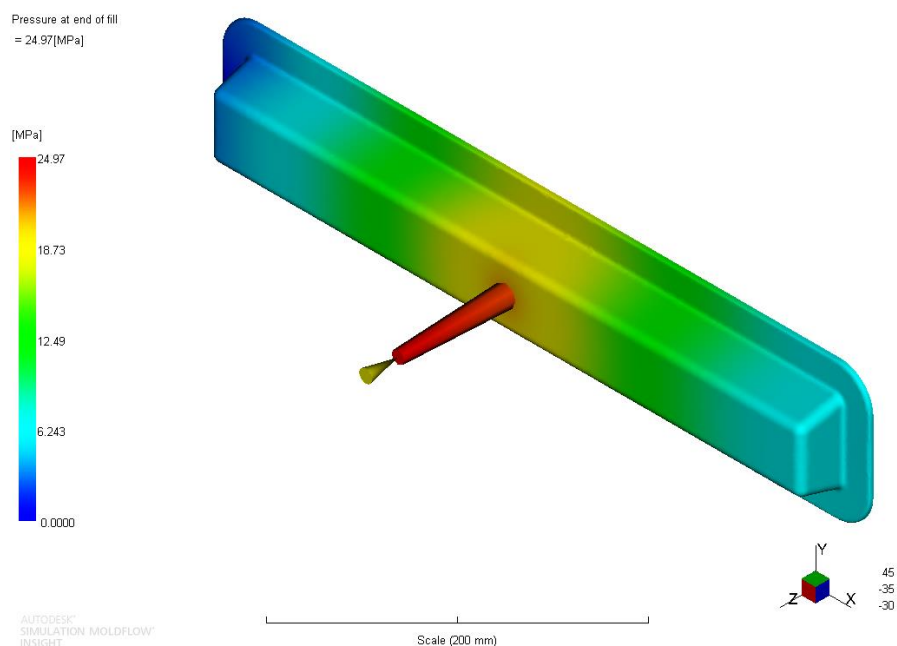
Figure 14. Distribution of pressure at the end of fill predicted for the 2.8-mm, 30wt% LCF/PA66 complex part with ribs – Acceptable level of the maximum pressure at the end of fill was found.
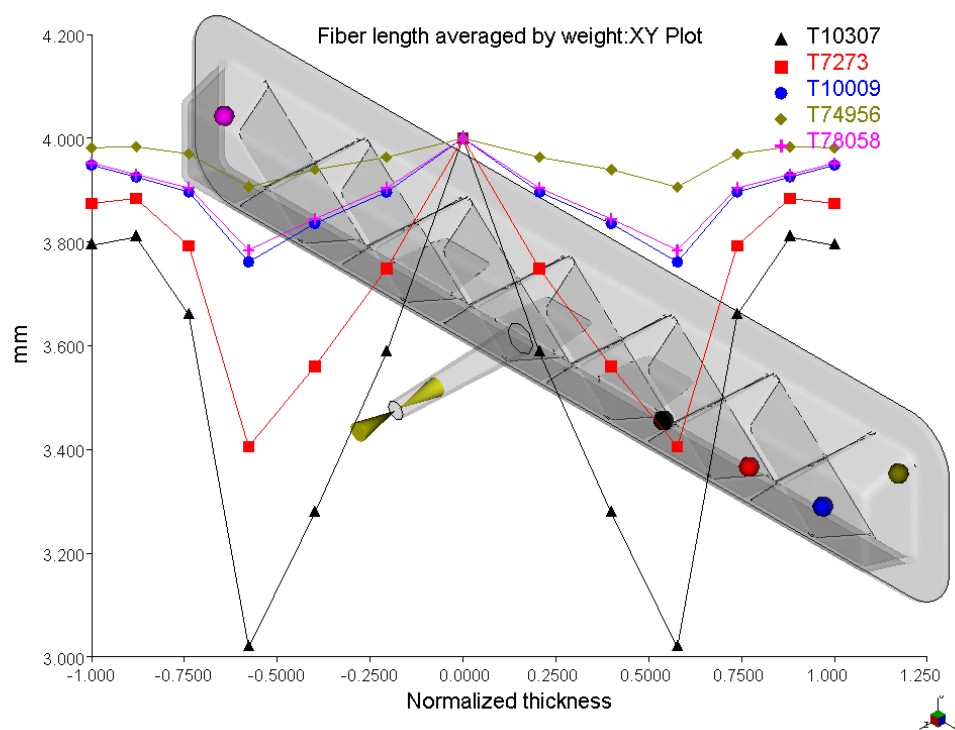

Figure 15. Predicted weight-average fiber lengths for the 2.8-mm, 30wt% LCF/PA66 complex part with ribs. The various locations selected on the part shows lengths exceeding the 1-2 mm range.
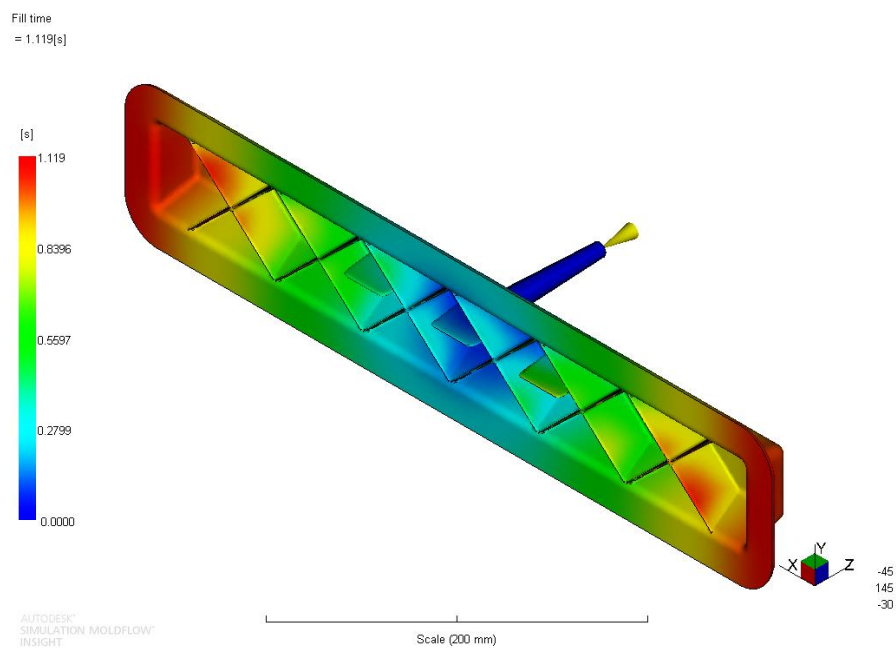
Figure 16. Fill time predicted for the 2.8-mm, 30wt% LCF/PP complex part with ribs – successful mold filling was predicted.
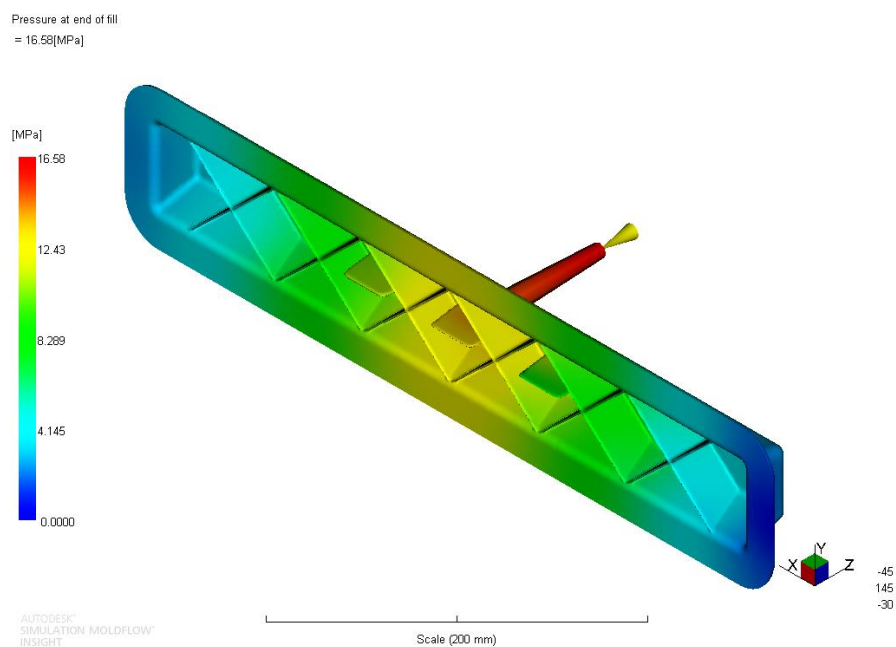

Figure 17. Distribution of pressure at the end of fill predicted for the 2.8-mm, 30wt% LCF/PP complex part with ribs – Acceptable level of the maximum pressure at the end of fill was found.
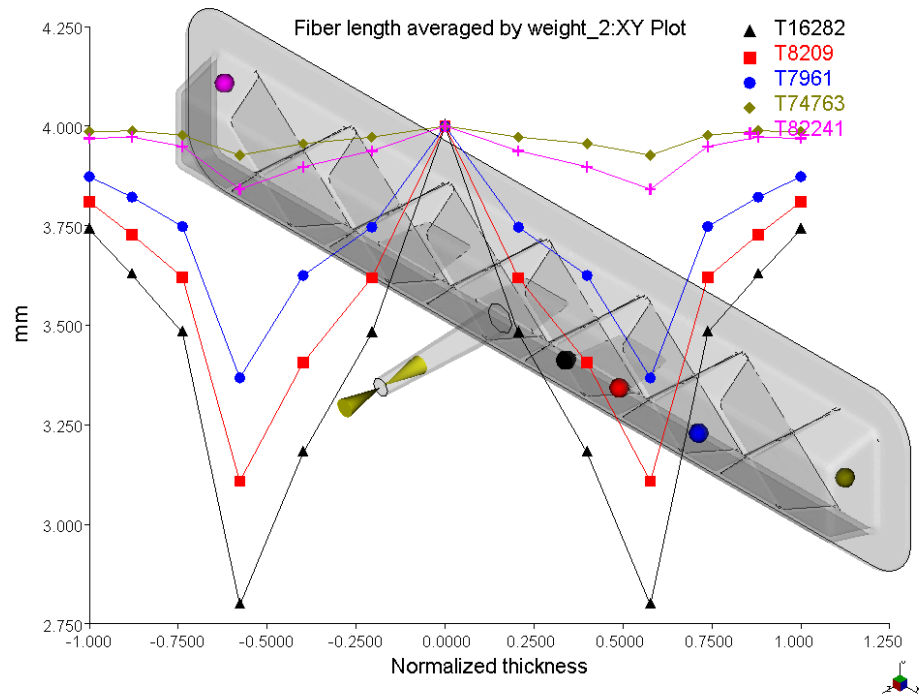
Figure 18. Predicted weight-average fiber lengths for the 2.8-mm, 30wt% LCF/PP complex part with ribs. The various locations selected on the part shows lengths exceeding the 1-2 mm range.

4.5 *Implementation and Improvements of Process Models in ASMI (Autodesk)*

Fiber Length Distribution Prediction by Proper Orthogonal Decomposition modes.

Autodesk has been working on implementing the new fiber length distribution (FLD) model based on an unbreakable length assumption with Reduced Order Modeling (ROM) by the Proper Orthogonal Decomposition (POD) approach in the mid-plane, dual-domain and 3D solvers. The recent focus of this work has been on removing the need for a preliminary snapshot analysis to determine the POD modes. The snapshot analysis previously used for this had required a long computation time and large computation memory while running the full flow and FLD models to pre-determine the POD modes for the use in the ROM scheme. The need for the snapshot analysis has been successfully removed by using a dynamic look-up table that covers a wide spectrum of shear-rate and viscosity variations in the analysis. It has been found in 3D analysis testing that the POD approach can predict FLD results which reasonably match those of the full model as illustrated in Figures 19 and 20.
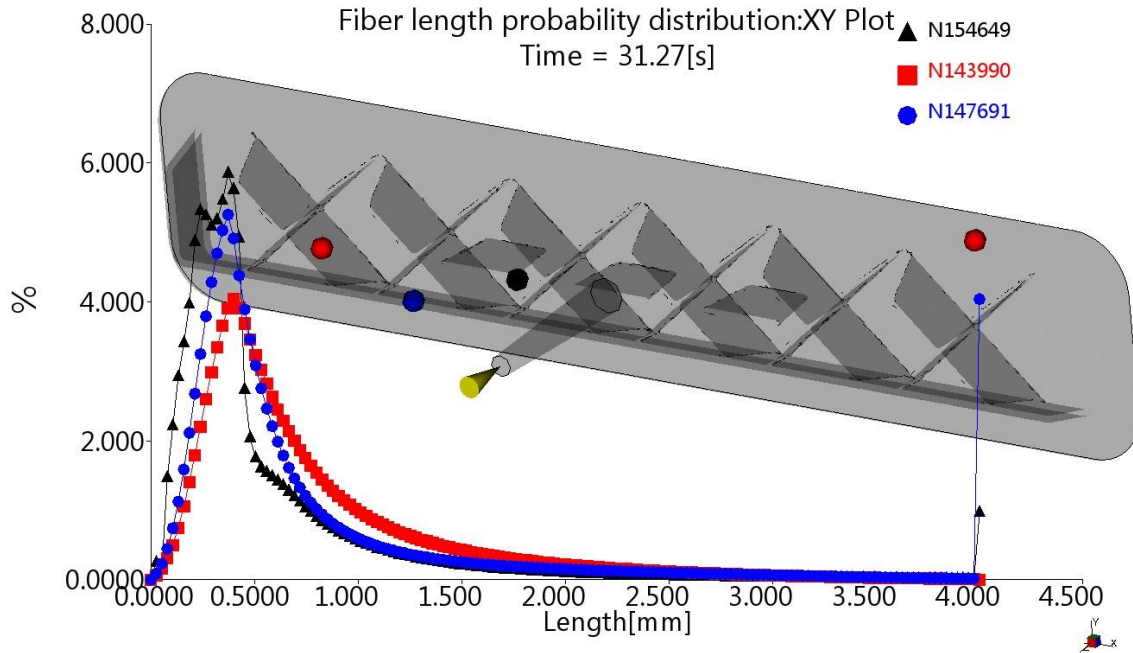
Figure 19. 3D Analysis-predicted FLD result for the complex part using the full fiber breakage model based on unbreakable length: 150 segments, drag coefficient, $D_g = 3.0$, shear rate constant, $C_b = 0.02$, and probability profile control factor, S=0.25 .
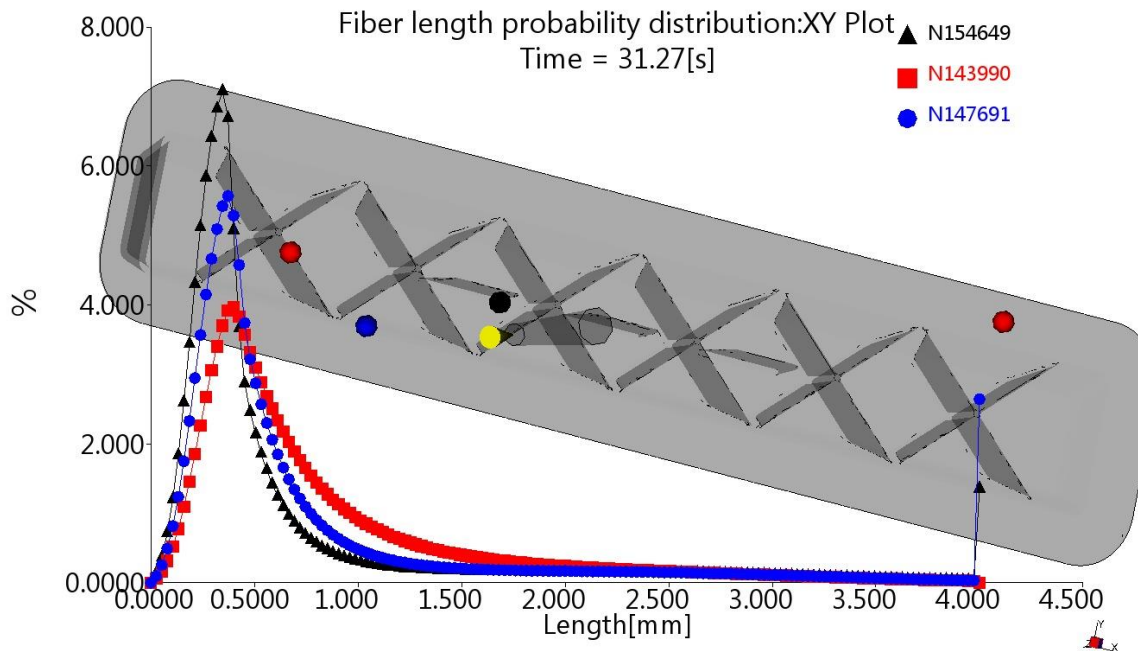

Figure 20. 3D Analysis-predicted FLD result for the complex part using *5 POD modes of the fiber breakage model based on unbreakable length*: 150 segments, $D_g = 3.0$, $C_b = 0.02$, S=0.25.

Figure 21, shows preliminary FLD results obtained for a mid-plane model calculation of an edge-gated plaque comparing the full fiber breakage model with 150 segments to the results predicted using 5 POD modes with 150 segments. The peak length probability values below 1 mm are under predicted with the POD method compared to the full model.
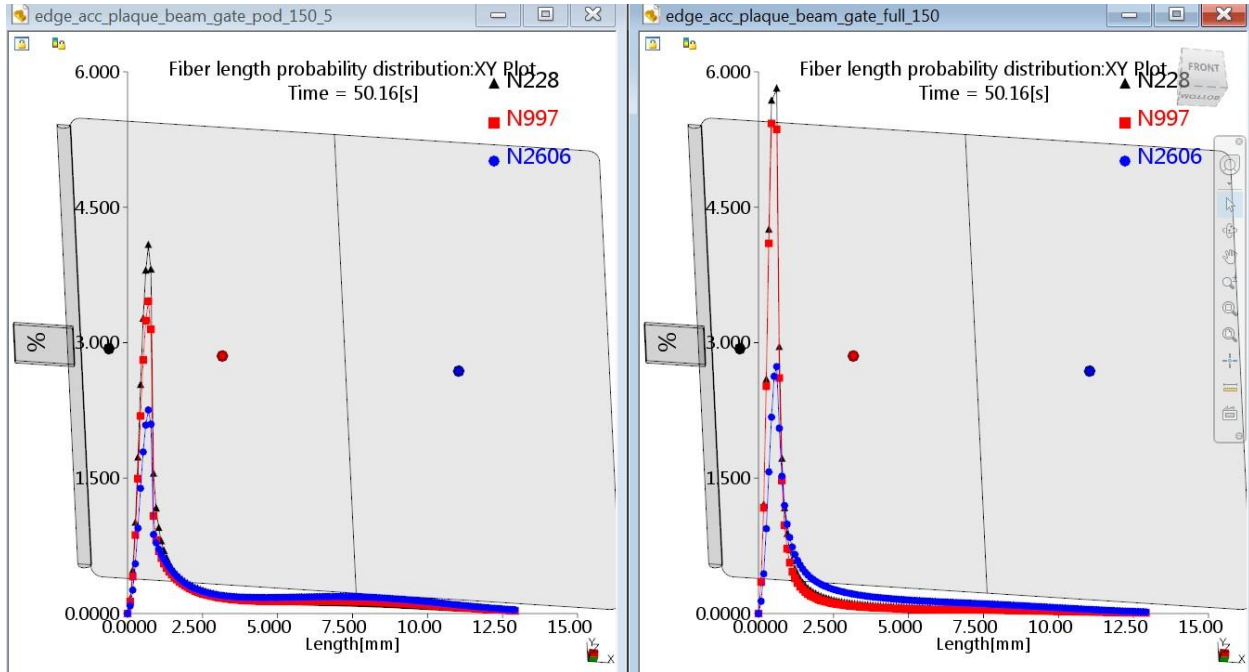

Figure 21. Accuracy comparison with a mid-plane mesh model: (Left) 150 Segments with 5 POD modes − (Right) Full Model with 150 Segments.

The computation memory required when using ROM with 5 POD modes and the full FLD model are compared in Table 13 for a dual-domain analysis of the complex part with 150 length segments in the FLD distribution. The memory required for the FLD calculation was reduced by 61% when ROM with 5 POD modes is used.

Analysis	Total Memory Required (MBytes)	Memory for FLD Calculation (MBytes)
Flow analysis without FLD calculation	1739	0
Flow with full FLD model	5387	3648
Flow with POD FLD model	3149	1410

Table 13. Memory usage of dual-domain flow and FLD calculation

However, as illustrated in the preliminary results shown in Figures 19, 20, and 21 the ROM approach is currently yielding results which can be somewhat different to the full model. We continue to examine these differences to further improve the simulation with POD modes and determine the minimum number of POD modes required for accurate solution. Further memory usage reductions may also be possible.
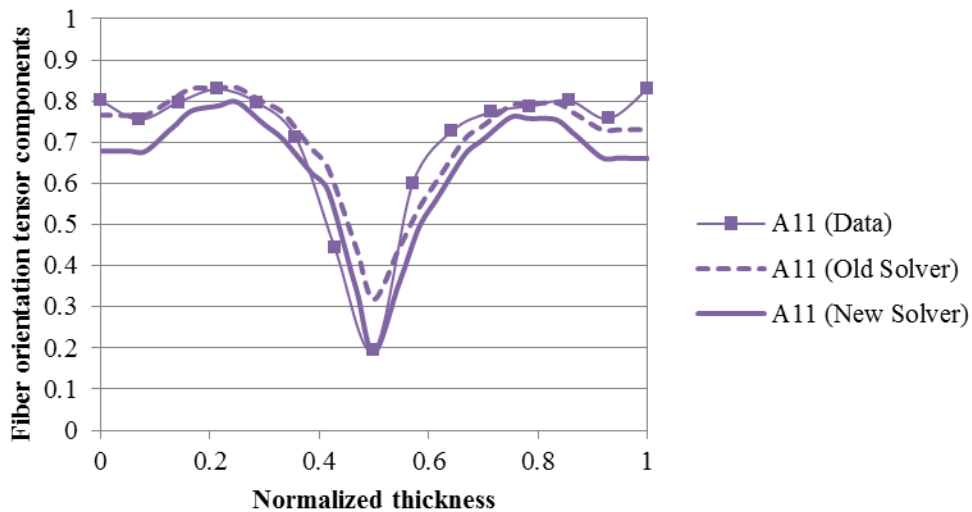
Fiber Orientation Prediction Improvements in the 3D Solver

Autodesk has also focused on improving the fiber orientation prediction by the reduced strain closure (RSC) model in *3D analysis*. The RSC model is used with the anisotropic rotary diffusion (ARD) model to predict the fiber orientation for long carbon-fiber composites. Previous comparisons to experimental data indicate that ASMI is able to reasonably predict the orientation component in the flow direction, but tends to over-predict orientation in the thickness direction and hence under-predict the orientation component in the cross-flow direction. Also the orientation near the mid-thickness plane is nearly always predicted to be fully random, regardless of the flow geometry, processing conditions and materials.

The RSC model has been carefully studied and the implementation has been improved, especially near the gate region, where the elongation flow is dominant as the melt polymer enters the cavity. The new ASMI 3D RSC solver have been tested for a number of injection-molded cases with short-fiber composites, and the fiber orientation prediction shows good agreement with most experimental data. Two example cases are presented in Figures 22 and 23. The improved RSC 3D solver provides much better prediction of the orientation components in the cross-flow direction and better agreement with experiment. The next steps will be to create ASMI 3D models for the PlastiComp plaques and validate the predictions of the 3D ARD-RSC model with the measured long carbon fiber orientation data.
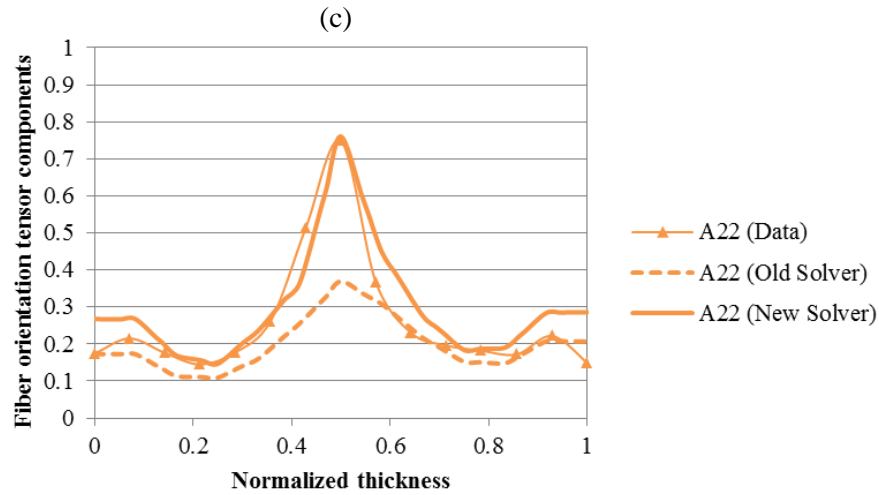

(a)

(b)

(c)

Figure 22. Comparison of fiber orientation data with ASMI predictions in the Delphi 90-mm long x 80-mm wide x 3-mm thick plaque: (a) 3D model; (b) orientation component in the flow direction; (c) orientation component in the cross-flow direction. The measured data are from Ref. [5]..
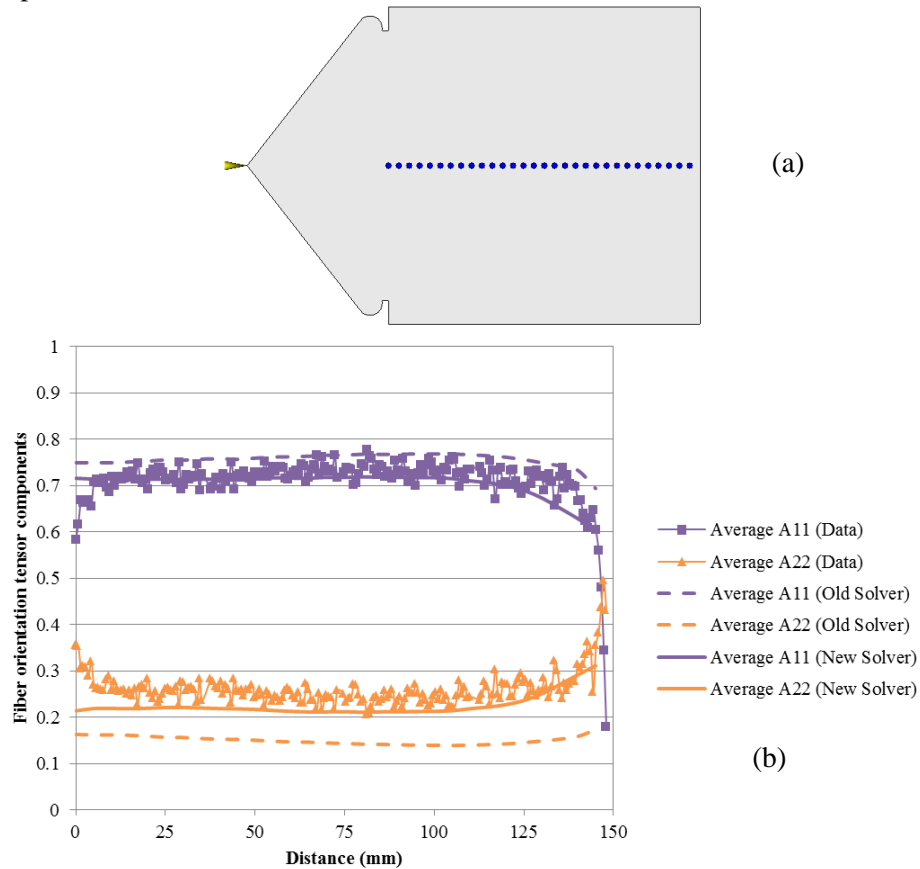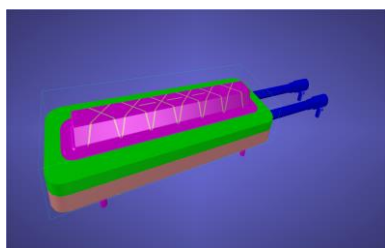

(a)

(b)

Figure 23. Comparison of fiber orientation data with ASMI predictions in the BASF 150-mm x 150-mm x 3-mm thick plaque: (a) 3D model and measurement locations; (b) orientation components in the flow and cross-flow directions. Fiber orientation is averaged through the thickness. The measured data were provided by BASF SE (Germany).

21

4.6 Complex Part Molding Preparation (Magna)

For the fourth quarter, Magna Exteriors molded plaques from 50wt% LCF/PP and 50wt% LCF/PA66 materials received from Plasticomp. The purpose of running the plaques was to obtain machine purgings from Magna's 200-Ton Injection Molding machine targeted to mold the complex part. The machine purgings (purge materials) were sent to Purdue University on July 25th for fiber length distribution comparison between the machine purge materials from Plasticomp, Autodesk and Magna. Edge-gated 8"x8" molded plaques were tested for physical properties by Magna's Product and Process Development Lab.

Magna participated in conference call discussions and project updates as well as attended the face-to-face meeting at Purdue University on August 6-7, 2014. Follow-up discussions pertaining to project timing and issues regarding fiber length measurements at Purdue were key topics requiring follow-up conference calls and correspondence. Establishing the test matrix and criteria for go/no-go assessment necessitated conference calls and Magna's input to the team regarding recommendations and agreement on modifying the complex part trial plan to switch from 50% LCF PP and 50% LCF PA66 to 30% LCF PP and 30% LCF PA66. Establishment of wall stock recommendation for the complex part that will provide acceptable process conditions and prediction for retaining average fiber length of 1-2 mm is the next critical step providing go/no-go targets are met. Tool kick-off will be delayed until go/no-go assessment is finalized. Wall stock thickness has been established by filling analysis of the complex 3D part.

- New mold will be single cavity tool designed for 200T Engel IMM
- Insert will be installed into mold base
- Cavity surface will be cut to desired wall thickness as determined by mold filling analysis
- Insert will be interchangeable with non-rib version

Mold Base

Figure 24. Schematic picture showing Magna's tool to mold the complex 3D part.

5. Publications/Presentations

None

6. Patents

None

7. Future Plans

Fiber orientation and fiber length distribution data from locations A, B, and C in composite plaques representing variations in key material and molding parameters will be used to validate ASMI fiber orientation and fiber length predictions for these parameters toward completion of a go/no-go list of validations. Agreement within 15% between mechanical performance values in terms of the principal elastic tensile and flexural moduli calculated from the experimentally determined and computed fiber orientation and length data for the 2D plaques on the go/no-go list will enable transition of the project to focus on the 3D complex part. When the project passes the go/no-go decision point Magna will kick off the tooling for the complex 3D part and PlastiComp will produce carbon fiber-filled materials to be used for part molding.

8. Budgetary Information

COST PLAN/STATUS

	Budget Period 1								Budget Period 2							
	Q1		Q2		Q3		Q4		Q1		Q2		Q3		Q4	
Baseline Reporting Quarter	9/11/2012 - 12/31/2012		1/1/2013 - 3/31/2013		4/1/2013 - 6/30/2013		7/1/2013 - 9/30/2013		10/1/2013 - 12/31/2013		1/1/2014 - 3/31/2014		4/1/2014 - 6/30/2014		7/1/2014 - 9/30/2014	
	Q1	Cumulative Total	Q2	Cumulative Total	Q3	Cumulative Total	Q4	Cumulative Total	Q1	Cumulative Total	Q2	Cumulative Total	Q3	Cumulative Total	Q4	Cumulative Total
Baseline Cost Plan																
Federal Share	$6,808	$6,808	$8,000	$14,808	$238,289	$253,097	$238,288	$491,385	$127,409	$618,794	$127,409	$746,203	$127,409	$873,612	$127,409	$1,001,021
Non-Federal Share	$0	$0	$0	$0	$285,177	$285,177	$285,177	$570,354	$127,867	$698,221	$127,867	$826,088	$127,867	$953,955	$127,867	$1,081,822
Total Planned	$6,808	$6,808	$8,000	$14,808	$523,466	$538,274	$523,465	$1,061,739	$255,276	$1,317,015	$255,276	$1,572,291	$255,276	$1,827,567	$255,276	$2,082,843
Actual Incurred Cost																
Federal Share	$6,808	$6,808	$2,536	$9,344	$743	$10,087	$418	$10,505	$62,859	$73,365	$117,143	$190,508	$87,207	$277,715	$90,514	$368,229
Non-Federal Share	$0	$0	$0	$0	$0	$0	$0	$0	$178,823	$178,823	$219,222	$398,045	$160,040	$558,085	$223,162	$781,247
Total Incurred Costs	$6,808	$6,808	$2,536	$9,344	$743	$10,087	$418	$10,505	$241,683	$252,188	$336,365	$588,553	$247,247	$835,800	$313,676	$1,149,476
Variance																
Federal Share	$0	$0	$5,464	$5,464	$237,546	$243,009	$237,870	$480,879	$64,550	$545,429	$10,266	$555,695	$40,202	$595,897	$36,895	$632,792
Non-Federal Share	$0	$0	$0	$0	$285,177	$285,177	$285,177	$570,354	-$50,956	$519,398	-$91,355	$428,043	-$32,173	$395,870	-$95,295	$300,575
Total Variance	$0	$0	$5,464	$5,464	$522,723	$528,186	$523,047	$1,051,233	$13,593	$1,064,827	-$81,089	$983,738	$8,029	$991,767	-$58,400	$933,367

9. References

1. Phelps JH. (2009). "Processing-Microstructural Models for Short- and Long-Fiber Thermoplastic Composites," PhD Thesis, University of Illinois at Urbana-Champaign, Urbana, IL 61801.
2. Phelps JH and CL Tucker III. 2009. "An Anisotropic Rotary Diffusion Model for Fiber Orientation in Short- and Long-Fiber Thermoplastics," *Journal of the Non-Newtonian Fluid Mechanics*, 156(3):165-176.
3. Advani S and CL Tucker III. 1987. "The Use of Tensors to Describe and Predict Fiber Orientation in Short-Fiber Composites." Journal of Rheology, 31: 751-784.
4. Nguyen BN et al. (2014). "Mold Filling Pre-Analysis of the 3D Complex Part – Milestone Report." PNNL-23772.
5. Wang, J. (2007). "Improved Fiber Orientation Predictions For Injection-molded Composites." Ph.D. Thesis, University of Illinois at Urbana-Champaign, Urbana, IL.